NATIONAL ADVISORY COMMITTEE FOR AERONAUTICS

TECHNICAL NOTE

No. 1481

DIAGONAL TENSION IN CURVED WEBS

By Paul Kuhn and George E. Griffith

Langley Memorial Aeronautical Laboratory
Langley Field, Va.

Washington
November 1947

NATIONAL ADVISORY COMMITTEE FOR AERONAUTICS

TECHNICAL NOTE No. 1481

DIAGONAL TENSION IN CURVED WEBS

By Paul Kuhn and George E. Griffith

SUMMARY

The engineering theory of incomplete diagonal tension in plane webs presented in NACA TN No. 1364 is generalized in order to make it applicable to curved webs. Comparisons are given between calculated and experimental results for a number of stiffened cylinders subjected to torsional loads. The results indicate that the theory predicts the stresses to about the same accuracy for curved webs as for plane webs. The failing stresses in the stringers in curved webs were predicted conservatively in all cases.

INTRODUCTION

Aeronautical practice in the design of stiffened sheet-metal structures has long been to permit buckling of the sheet except for such restrictions as may be imposed by aerodynamic considerations. When the sheet is subjected essentially to shear forces, the state of stress that exists after buckling has taken place is known as diagonal tension. The theory of diagonal tension in plane (flat) webs was developed in considerable detail by Wagner (reference 1) for the theoretical limiting case of fully developed diagonal tension. For the practical and more general case of partly developed plane diagonal tension, theories of varying scope and refinement have been given by a number of authors. The engineering theory of incomplete plane diagonal tension given in reference 2 is semiempirical but is simple to use and has a wide scope.

A theory of diagonal tension in curved webs has also been given by Wagner, again for the theoretical limiting case of fully developed diagonal tension (reference 3). Because the curvature introduces several complications, Wagner was forced to make more restrictive assumptions in the theory of curved webs than in the theory of plane webs. These additional complications have greatly retarded the development of a theory of incomplete curved diagonal tension. The first attempt to develop such a theory was made by Wagner in reference 3, where he suggested the assumption that the shear stress in excess of

the critical value τ_{cr} is carried by diagonal tension. The resulting theory is known to be unsatisfactory for plane sheet and consequently is inacceptable as basis of a general theory. Schapitz proposed a semiempirical theory (reference 4) but did not furnish the empirical data required to develop it. His theory is also based on an assumption essentially equivalent to that of reference 3, although Schapitz states in passing that a different physical action is quite conceivable.

In the present paper, a semiempirical engineering theory of curved diagonal tension is obtained by generalizing the theory of plane diagonal tension presented in reference 2.

SYMBOLS

d spacing of rings, inches

h spacing of stringers, inches

k diagonal-tension factor

q shear flow, pounds per inch

t thickness, inches (without subscript signifies thickness of web)

A cross sectional area, square inches

D flexural stiffness of panel per unit length $\left(\frac{Et^3}{12(1-\mu^2)}\right)$, inch-pounds

E Young's modulus of elasticity, ksi

R radius of curvature, inches

Z curvature parameter $\left(\frac{h^2}{Rt}\sqrt{1-\mu^2} \text{ or } \frac{d^2}{Rt}\sqrt{1-\mu^2}\right)$ (Use whichever is smaller of h or d.)

α angle of diagonal tension, degrees

ϵ normal strain

μ Poisson's ratio

σ normal stress, ksi

τ shear stress, ksi

ρ radius of gyration of cross section, inches

Δ correction factor for allowable shear stress

Subscripts:

all allowable

cr critical

e effective

max maximum

DT diagonal tension

PDT pure diagonal tension

RG ring

S shear

ST stringer

Special Combinations:

k_s critical-shear-stress coefficient, established by geometry of panel and type of edge support

σ_o "basic" allowable compressive stress for forced crippling of stiffeners (valid for stresses below proportional limit of material), ksi

τ^*_{all} "basic" allowable shear stress, ksi

ENGINEERING THEORY OF CURVED DIAGONAL TENSION

State of Stress before Buckling of Sheet and Calculation of Buckling Stress

When a stiffened cylinder is subjected to torque loads applied at the ends of the cylinder, a uniform shear flow q is generated in the sheet (except near the ends). No stresses exist in the stiffeners or rings until the sheet begins to buckle.

According to reference 5, the stress at which the sheet buckles is given, if h is smaller than d, by the formula

$$\tau_{cr} = \frac{k_s \pi^2 D}{th^2} = \frac{k_s \pi^2 E h^2}{12R^2 Z^2} \qquad (1)$$

If d is smaller than h, then d replaces h in the formula. The coefficient k_s is given in figure 1 as a function of Z. This theoretical formula assumes that the edges of the panel are simply supported, whereas actually the edges of panels are riveted to stiffeners or rings. However, the agreement between experimentally observed buckling stresses and stresses predicted by formula (1) is good, as shown in reference 5 and again confirmed by the tests made in the present investigation. Formula (1) was therefore used to evaluate the tests to be described subsequently herein and is recommended for use in stress analysis. A reduction factor might be necessary when the thickness of the stiffener (or the ring) is appreciably less than the thickness of the sheet. For flat sheet, such a reduction factor was given in reference 2. For sheet with appreciable curvature, the reduction appears to be less than that for flat sheet, but the available data are insufficient to warrant even tentative recommendations for a reduction factor. A substantial reduction factor is probably necessary when the sheet is very thin ($t < 0.020$ in.).

State of Stress after Buckling of Sheet

When the torque increases beyond the magnitude that produces a shear stress equal to τ_{cr} in the sheet, the sheet buckles and begins to carry the shear flow partly in diagonal tension. This action produces compressive forces in the stringers and in the rings, and the corresponding stress system may be considered as the primary stress system in the twisted cylinder. The stiffeners, and to a lesser extent the rings, are also subjected to bending loads; the stresses caused by these bending actions may be considered as a secondary stress system and will not be treated in this paper. Deviations of the sheet stress from a uniform average stress might also be classified as belonging to the secondary stress system.

The engineering theory of plane diagonal tension given in reference 2 is based on the assumption that the shear flow q acting on the sheet can be divided into a diagonal-tension part q_{DT} and a shear part q_S by writing

$$\begin{aligned} q_{DT} &= kq \\ q_S &= (1 - k)q \end{aligned} \tag{2}$$

The fraction k specifies the degree to which the diagonal tension is developed; when $k = 0$, there is no diagonal-tension action, only shear action in the sheet; when $k = 1$, the diagonal tension is fully developed and the laws of pure diagonal tension apply. The compressive forces in the stringers and rings are caused by the diagonal-tension component kq of the total shear flow q.

The value of k is given by the empirical formula

$$k = \tanh\left[\left(0.5 + 300\frac{t_d}{Rh}\right)\log_{10}\frac{\tau}{\tau_{cr}}\right] \tag{3}$$

When $R \longrightarrow \infty$, the formula reduces to that given in reference 2 for plane diagonal tension. When the value of the constant $300\frac{t_d}{Rh}$ has been computed, the value of k for any desired value of τ/τ_{cr} may be read from figure 2, which is a graphical presentation of formula (3).

According to the theory of reference 2, the stress in a stringer is given by

$$\sigma_{ST} = -\frac{k\tau \cot \alpha}{\frac{A_{ST}}{ht} + 0.5(1 - k)} \tag{4}$$

and the stress in a ring by

$$\sigma_{RG} = -\frac{k\tau \tan \alpha}{\frac{A_{RG}}{dt} + 0.5(1 - k)} \tag{5}$$

For convenience, the minus signs on σ_{ST} and σ_{RG} will be omitted in this paper. In stress analysis, they must be retained to ensure the proper combination of these stresses with others not arising from diagonal-tension action.

For plane diagonal tension, the theoretical calculations made by Levy and his collaborators and discussed in reference 2 show that the compressive stress in a stiffener is not uniform but has a minimum value at the ends of the stiffener and a maximum value in the middle. The maximum value is used to estimate the resistance of the stiffener to forced crippling induced by the shear buckles in the sheet. For curved diagonal-tension fields, the maximum stresses may be estimated by means of the formulas

$$\sigma_{ST_{max}} = \sigma_{ST}\left(\frac{\sigma_{ST_{max}}}{\sigma_{ST}}\right)$$

$$\sigma_{RG_{max}} = \sigma_{RG}\left(\frac{\sigma_{RG_{max}}}{\sigma_{RG}}\right)$$

where the values of σ_{ST} and σ_{RG} are those obtained from formulas (4) and (5), respectively, and the ratios $\frac{\sigma_{ST_{max}}}{\sigma_{ST}}$ and $\frac{\sigma_{RG_{max}}}{\sigma_{RG}}$ are

obtained from figure 3, which is figure 10 of reference 2. The theoretical calculations on which figure 3 is based were made for plane beams in which the ratio of flange area to web area is very large. This condition is generally not fulfilled for cylinders; the accuracy of the results obtained when figure 3 is used for cylinders may therefore be expected to be less than when it is used for plane beam webs.

The angle α between a generatrix of the cylinder and the direction of the diagonal tension is given by the formula

$$\tan^2\alpha = \frac{\epsilon - \epsilon_{ST}}{\epsilon - \epsilon_{RG} + \frac{1}{24}\left(\frac{h}{R}\right)^2} \tag{6}$$

where ϵ is the strain in the sheet along the direction of the diagonal tension, $\epsilon_{ST} = \frac{\sigma_{ST}}{E}$ is the strain in the stringer, and $\epsilon_{RG} = \frac{\sigma_{RG}}{E}$ is the strain in the ring. The strain ϵ in the sheet is given by the formula

$$\epsilon = \frac{\tau}{E}\left[\frac{2k}{\sin 2\alpha} + \sin 2\alpha\,(1 - k)(1 + \mu)\right] \tag{7}$$

which can be evaluated with the aid of figure 4. (Note that ϵ_{ST} and ϵ_{RG} are inherently negative when they arise from the stresses σ_{ST} and σ_{RG} given in formulas (4) and (5).)

Formulas (4), (5), and (7) are analogous to the corresponding formulas for plane diagonal tension. Formula (6) differs from the corresponding formula for plane diagonal tension by the term containing R, which disappears for flat sheet. This term constitutes an allowance for the fact that the circular cylinder after buckling tends to approach a polygonal cylinder, the sheet pulling flat from stringer to stringer (reference 3). The coefficient 1/24 is the theoretical coefficient for fully developed diagonal tension. Theoretically, the coefficient should be less than 1/24 until the ratio of applied load to buckling load approaches infinity. Test observations indicated, however, that the flattening proceeds very rapidly, and trial calculations showed that the best agreement with the test data was obtained by using the full value of the coefficient. The use of the full value of the

coefficient immediately after buckling is also supported qualitatively by the test observation, contained in reference 6, that the shear strain of a curved sheet panel generally shows a large instantaneous increase when buckling takes place.

Because formulas (4) to (7) are interdependent, they must be solved by successive approximation. A value of α is estimated; ϵ_{ST} and ϵ_{RG} are calculated from formulas (4), (5), and (7), and the resulting values are used to calculate an improved value of α by means of formula (6); the process is repeated until the calculated value of α is sufficiently close to the assumed value. Normally, no more than three cycles of the computation are necessary.

A first estimate of the angle α may be made by means of the formula

$$\alpha \approx \alpha_{PDT} \frac{\alpha}{\alpha_{PDT}} \tag{8}$$

with α_{PDT} taken from figure 5 and the ratio $\frac{\alpha}{\alpha_{PDT}}$ from figure 6. The angle α_{PDT} is the inclination that the folds would take at the given load if the sheet were in a state of pure diagonal tension, a condition that could be realized theoretically if the sheet were divided into a large number of laminae free to slide over each other. (Such a division would destroy the bending stiffness of the sheet without affecting the extensional stiffness.) The curve shown in figure 5 was obtained by solving a transcendental equation for α_{PDT} that can be obtained from equations (4) to (7) on the assumption that the stiffening ratios A_{ST}/ht and A_{RG}/dt are equal. In practice, these ratios will probably not be equal, but the curve may be used to obtain a first approximation. The curve shown in figure 6 is computed for one specific cylinder in which both stiffening ratios are equal to unity. This curve lies about in the middle of a scatter band formed by the curves for a number of cylinders within the practical range of proportions. For the cylinders and curved-web beams analyzed in the experimental part of the present investigation, the angle α estimated by means of formula (8) differed from the angle calculated by successive approximation by less than 2° in most cases, with a maximum difference of about 3°.

Ultimate Strength of Sheet

The ultimate strength of the sheet can be estimated by means of the empirical formula

$$\tau_{all} = \tau^*_{all} (0.65 + \Delta) \tag{9}$$

where τ^*_{all} is a "basic" allowable shear stress, taken from figure 7 for 24S-T aluminum alloy, and

$$\Delta = 0.3 \tanh \frac{A_{RG}}{dt} + 0.1 \tanh \frac{A_{ST}}{ht} \tag{10}$$

The value of Δ can be obtained from the graph in figure 8.

The chart for τ^*_{all} (fig. 7) was constructed as follows: The top curve for $\alpha_{PDT} = 45^\circ$ is the empirical curve for flat sheet and was taken from figure 14(a) of reference 2. Values of τ^*_{all} for fully developed diagonal tension ($k = 1$) were computed for various values of α_{PDT} on the basis of the fundamental formula for sheet tensile stress

$$\sigma_{PDT} = \frac{2\tau}{\sin 2\alpha_{PDT}} \tag{11}$$

The curve of τ^*_{all} against k was then constructed for each value of α_{PDT} on the assumption that the difference between the curve sought and the curve for $\alpha_{PDT} = 45^\circ$ was proportional to k. Equation (10) for the correction factor Δ is an empirical expression based on an analysis of the available test data.

Ultimate Strength of Stringers

Reference 2 lists four conceivable types of stiffener failures in plane shear webs as follows:

(1) Column failure
(2) Forced-crippling failure
(3) Natural-crippling failure
(4) General elastic instability of entire system

The same types of failure are conceivable in curved shear webs. In curved webs, the stiffening system is probably always located on the inside of the curve; the following discussion is therefore confined to single stringers and rings.

Column failure.- Column failure may be expected to take place when the stringer stress σ_{ST} equals the column-failing stress of the stringer section as determined for a slenderness ratio of $d/2\rho$. This rule given in reference 2 for plane webs is consistent with the consideration that the stringers in curved webs will probably tend to buckle inward as a result of the radial force exerted by the diagonal tension, and the bracing action exerted by a plane web (reference 2) is then absent; on the other hand, the stringers are usually continuous over several bays and may, therefore, be considered as fixed at each ring. (When the stringer is not continuous, as in an end bay, an appropriate reduction must, of course, be made in the allowable stress.) Moore and Wescoat suggest in reference 7 that the allowable stress be taken as that obtained by testing the stringer flat-ended, with a length equal to the ring spacing. Carefully made flat-end tests are known to give restraint coefficients of 3.75 or somewhat higher. The rule of Moore and Wescoat is therefore slightly more conservative than that just given, which implies a restraint coefficient of 4.0, but the difference is well within the probable scatter limits of diagonal-tension tests; the direct use of test data implied by the rule also ensures that twisting failure of the stringers is taken into account, a factor that might be overlooked when column curves are used.

Forced-crippling failure.- Failure of a stringer initiated by forced crippling may be expected to take place when the maximum stringer stress $\sigma_{ST_{max}}$ becomes equal to the allowable stress given by the empirical formula

$$\sigma_o = 28k \sqrt{\frac{t_{ST}}{t}} \tag{12}$$

If σ_o exceeds the proportional limit, the compressive stress corresponding to the strain σ_o/E should be used as allowable value. If $k < 0.5$, an effective value defined by

$$k_e = 0.15 + 0.7\,k \tag{13}$$

should be used in formula (12). Because the allowable stress is a function of the load, the predicted failing load must be obtained as the point of intersection of the curve of stringer stress $\sigma_{St_{max}}$ against load and the curve of allowable stringer stress σ_o against load.

All of these formulae for forced crippling are taken directly from reference 2.

Natural-crippling failure.- The term "natural-crippling failure" is used herein to denote a failure of the stiffener caused by compressive stresses alone. Failure by forced crippling probably always takes place before failure by natural crippling can occur, but the existing knowledge is too limited to permit a positive statement on this question.

General elastic instability.- An empirical formula for general elastic instability was given recently in reference 8.

Ultimate Strength of Rings

Only a few ring failures were observed in the available tests, and they were definitely secondary failures; consequently, no procedure for strength analysis can be recommended at present. The following suggestions may be made:

(1) Rings riveted to the skin are susceptible to forced crippling and should be checked by formula (12).

(2) Rings notched out to pass the stringers through should be checked to insure that the net section of the notch is safe against local crippling. (The net section must carry the entire compressive force acting in the ring and has therefore a much higher stress than the full section of the ring.)

EXPERIMENTAL INVESTIGATION

Test Specimens

The test specimens consisted of eight 30-inch-diameter cylinders of 24S-T aluminum alloy, reinforced transversely by rings and longitudinally by 12 equally spaced stringers. Double stringers were used on these cylinders in order that stringer bending stresses might be eliminated by suitable averaging of the strain readings. Detailed dimensions of the cylinders are given in table 1, and pertinent details of construction are shown in figures 9 and 10.

Additional test data were obtained from references 7 and 9 and from unpublished NACA data.

Test Procedure

Each cylinder was secured at one end to a rigid support while torque was applied at the other end through a steel frame loaded by a hydraulic jack. In order to insure uniform distribution of the load, a large circular steel head was attached to the loaded end of the cylinders. The weight of this steel head was counterbalanced so that the cylinders were not subjected to bending loads.

Stringer stresses were computed from measurements with Baldwin-Southwark SR-4 resistance-type wire strain gages, types A-1, A-5, and A-12, with gage lengths of 13/16, 1/2, and 1 inch, respectively. All gages were used in pairs, one gage on the outer flange of each component stringer, in order to eliminate (or minimize) the effects of local bending. A fairly large number of gages (an average of 58 per cylinder) were used at a number of stations over several bays so that a reasonable approximation to the average stringer stress would be obtained. Ring stresses were computed from measurements with SR-4 gages, types A-1 and A-12, applied to the ring web at the mean radius line of the ring.

Cylinder 7 was accidentally loaded before any gage readings were recorded to a point where small buckles appeared in the skin. As indicated in reference 10, the value of the buckling stress τ_{cr} was probably reduced a small amount (approximately 5 percent or less) by this preloading.

Cylinder 1 was loaded by a torsion jig that was found to have insufficient throw and started to bind at about 95 percent of the ultimate load. For the remaining tests, a new jig was used.

Results of Strain Measurements

Figure 11 shows the stringer stresses obtained from the strains measured on the 8 cylinders of the present investigation as well as the stresses computed by means of the proposed engineering theory. As mentioned in the section "Test Procedure", strains were measured by pairs of gages at about 29 stations in each cylinder. The average strain in any one pair of gages, multiplied by Young's modulus, represents the compressive stress in the stringer at that station, subject, however, to errors introduced by local buckling of the stringer. The lowest and the highest values of this stress for each cylinder are

indicated by the tick marks terminating the horizontal line drawn for each load. The over-all average (that is, the average for all 29 stations) is indicated by a circle. The agreement between the computed curves and the circles is consistently very close for the cylinders with square skin panels $\left(d = \frac{R}{2}\right)$; for the cylinders with long skin panels $(d = R)$, the agreement is not so consistent, although reasonably satisfactory except on cylinder 5. The horizontal lines with their tick marks show that individual stresses can differ greatly from the average value as the combined result of variation of compressive force along the length of the stringer, secondary bending, and local buckling.

The ring stresses measured on the eight cylinders are shown in figure 12. As mentioned previously, the strain gages were attached to the webs of the rings at the mean radius. Because the neutral axis does not coincide with the mean radius, and because the total number of gages used on the rings was relatively small, the measured ring stresses can be considered only as a rough approximation to the average compressive ring stress.

Stringer stresses for the cylinders tested by Moore and Wescoat (reference 7) are shown in figure 13. These cylinders had proportions similar to those of the cylinders tested in the present investigation; the main difference was that single stringers of inverted Ω-section were used (on the outside of the cylinder) instead of double stringers. The number of strain gages used in the tests of reference 7 was much smaller than in the present investigation. In addition, it must be remembered that rigid-body strain gages, such as the Whittemore gages used by Moore and Wescoat on specimens 20 and 21, measure not only the compressive strain but also the geometric shortening between gage points induced by bending deflection of the stringers. In view of these facts, the agreement between computed and measured stresses may be considered satisfactory.

Comparison of figures 11 to 13 with figure 17 of reference 2 indicates that the agreement between measured and calculated stiffener stresses is of the same order on cylinders as on plane-web systems.

Ultimate Strength of Sheet

Before the experimental evidence on the ultimate strength of sheets can be presented, the design chart of figure 7 requires some discussion.

As explained in the presentation of figure 7, the chart is derived from an empirical curve for flat sheet taken from reference 2. Inspection

of the relevant figures in reference 2 will show that two curves are given for each material, one for webs on which the rivet heads bear directly on the sheet and one for webs on which the rivet heads are separated from the sheet by heavy washers or by one leg of the flange angle. The curve for the first condition is about 10 percent lower than that for the second condition and was used as basis for deriving the curves of τ^*_{all} in figure 7, because the most common use of curved webs is on the outside of the aircraft structure where no washers would normally be used under the rivet heads. In all but one of the available tests, however, the second condition prevailed. In the cylinders used in the present investigation, the skin joints were underneath the double stringers shown in figure 10; in the curved-web beams described in reference 9, the edge of the web was sandwiched between the flange angle and a strap of aluminum alloy. Consequently, the test results were not evaluated on the basis of the chart given in figure 7, but on the basis of a similar chart derived from the appropriate (upper) curve for flat sheet given in reference 2.

The experimental data examined included the results from the present investigation and from references 7 and 9, some unpublished data on beams similar to those of reference 9 except that the rings were flat bars instead of formed Z-sections, and unpublished tests on two cylinders of 15-inch diameter. The construction of these two cylinders was such that the chart of figure 7 was applicable.

The data on the web failures experienced in the present investigation are given in table 2. (Predicted failing torques have been corrected to actual sheet properties.) If cylinder 1 is disregarded, the average ratio of actual to predicted strength is about 1.05, with a scatter of about ± 0.04. Since the indicated failing load on cylinder 1 was in error due to binding of the loading jig, the actual failing load was undoubtedly higher than the indicated one, although it is questionable whether the error was as large as 10 percent. It is possible, therefore, that the strength prediction would have been somewhat unconservative compared with the true ultimate strength.

On one of the 15-inch cylinders a web failure was experienced with a ratio of actual torque to predicted torque of 1.03.

For 11 web failures on beams such as those described in reference 9, the average ratio of actual to predicted strength was about 1.05, with a scatter of about ± 0.08. The scatter band for the beam tests is therefore twice as wide as for the present cylinder tests.

For the tests on plane-web beams discussed in reference 2, the ratio of actual to predicted strength was about 1.07 ± 0.06; the accuracy of strength prediction is therefore about the same for curved and for plane webs.

Not included in the analysis were two tests (one 13-inch cylinder and cylinder 15 of reference 7) in which sheet failure took place in an end bay. Tests of beams with plane webs indicate that it is very difficult to realize more than about 90 percent of the web strength unless the end bays are reinforced by doubler sheets, and much less may be realized unless the end uprights are very carefully proportioned. In cylinder 15 of reference 7, only 63 percent of the predicted strength was realized as a result of sheet failure in the end bay (table 2). The introduction of a torque into the end of a cylinder probably requires a doubler sheet if the full strength of the sheet is to be realized.

Ultimate Strength of Stringers

Table 2 gives ultimate torques predicted on the assumption that the stringers fail either by forced crippling or by column action. Comparison of the predicted with the actual failing torques, also given in the table, shows that the strength predictions were always conservative. The ratio of actual to predicted strength ranges from 1.06 to 1.89 for the cylinders in which the stringers failed. For a large number of tests on plane webs (reference 2), the average ratio was 1.2, and only in a very few tests was the ratio 1.4 exceeded appreciably. Table 2 shows three tests out of seven with a ratio appreciably larger than 1.4. This result indicates either that the predicted maximum stringer stresses in curved webs are too high or that the allowable stresses are higher than in plane web systems.

In passing, it may be noted that for all the cylinders in table 2 the calculations predicted correctly whether the failure would be stringer or sheet failure.

Checks for general elastic instability by the method of reference 8 showed that the cylinders of the present investigation had extremely large margins against failure of this type. For the cylinders of reference 7, the margins were smaller, but still positive, with a minimum margin of about 20 percent.

CONCLUSIONS

An engineering theory of (incomplete) curved diagonal tension, obtained by generalizing a previously published theory of plane diagonal tension, is presented together with pertinent test data. Analysis of the test data by the proposed theory indicates that, for curved webs,

1. The (primary) compressive stresses in the stiffeners and rings were computed by the theory with about the same accuracy as for plane webs.

2. The failing stresses of the sheet were predicted with about the same accuracy as for plane webs.

3. The failing stresses of the stringers were predicted conservatively in all cases, more conservatively and with more scatter than for plane webs.

Langley Memorial Aeronautical Laboratory
National Advisory Committee for Aeronautics
Langley Field, Va., August 15, 1947

REFERENCES

1. Wagner, Herbert: Flat Sheet Metal Girders with Very Thin Metal Web. Part I – General Theories and Assumptions. NACA TM No. 604, 1931. Part II – Sheet Metal Girders with Spars Resistant to Bending. Oblique Uprights – Stiffness. NACA TM No. 605, 1931. Part III – Sheet Metal Girders with Spars Resistant to Bending. The Stresses in Uprights – Diagonal Tension Fields, NACA TM No. 606, 1931.

2. Kuhn, Paul, and Peterson, James P.: Strength Analysis of Stiffened Beam Webs. NACA TN No. 1364, 1947.

3. Wagner, H., and Ballerstedt, W.: Tension Fields in Originally Curved, Thin Sheets during Shearing Stresses. NACA TM No. 774, 1935.

4. Schapitz, E.: Contributions to the Theory of Incomplete Tension Bay. NACA TM No. 831, 1937.

5. Batdorf, S. B., Stein, Manuel, and Schildcrout, Murry: Critical Shear Stress of Curved Rectangular Panels. NACA TN No. 1348, 1947.

6. Quick, A. W.: Untersuchung eines gekrümmten Zugblechträgers. Forschungsbericht Nr. 344, Flugtechnisches Institut an der Technischen Hochschule (Danzig), May 22, 1935.

7. Moore, R. L., and Wescoat, C.: Torsion Tests of Stiffened Circular Cylinders. NACA ARR No. 4E31, 1944.

8. Dunn, Louis G.: Some Investigations of the General Instability of Stiffened Metal Cylinders. VIII – Stiffened Metal Cylinders Subjected to Pure Torsion. NACA TN No. 1197, 1947.

9. Chiarito, Patrick T.: Some Strength Tests of Stiffened Curved Sheets Loaded in Shear. NACA RB No. L4D29, 1944.

10. Kuhn, Paul, and Levin, L. Ross: An Empirical Formula for the Critical Shear Stress of Curved Sheets. NACA ARR No. L5A05, 1945.

TABLE 1.- DIMENSIONS OF CYLINDERS

Cylinder	t (in.)	R (in.)	d (in.)	h (in.)	t_{ST} (in.)	t_{BG} (in.)	A_{ST} (sq in.)	A_{BG} (sq in.)
1	0.0248	15.04	15.00	7.87	0.052	0.061	0.230	0.197
2	.0266	15.03	7.50	7.87	.050	.064	.221	.202
3	.0265	15.02	15.00	7.86	.033	.063	.155	.198
4	.0266	15.02	7.50	7.86	.033	.068	.153	.216
5	.0393	15.03	15.00	7.87	.081	.104	.335	.320
6	.0394	15.05	7.50	7.88	.080	.104	.332	.317
7	.0428	15.04	15.00	7.87	.053	.102	.239	.318
8	.0399	15.06	7.50	7.88	.053	.102	.239	.321

NATIONAL ADVISORY
COMMITTEE FOR AERONAUTICS

TABLE 2.- ULTIMATE STRENGTHS

Cylinder	Predicted ultimate torques for failure by			Test		Test ultimate torque / Predicted ultimate torque		
	(1)	(2)	(3)					
	Stringer forced crippling (in.-kips)	Stringer bowing (in.-kips)	Sheet rupture (in.-kips)	Ultimate torque (in.-kips)	Failure observed	(4) (1) (a)	(4) (2) (a)	(4) (3) (a)
1	1010	1200	744	669	(3)	0.66	0.56	0.90
2	1010	1950	935	944	(3)	.93	.48	1.01
3	440	660	793	468	(1)	1.06	.71	.59
4	520	1060	933	732	(1)	1.41	.69	.78
5	1400	1950	1220	1261	(3)	.90	.65	1.03
6	1520	3400	1400	1528	(3)	1.01	.45	1.09
7	590	1400	1280	1113	(1)	1.89	.80	.87
8	950	2260	1410	1503	(1) and (3)	1.58	.67	1.07
[a]14	220	445	613	343	(1)	1.56	.77	.56
[a]15	520	690	635	398	(b)	.77	.58	.63
[a]20	470	400	601	442	(1)	.94	1.11	.74
[a]21	500	720	655	588	(1)	1.18	.82	.90

[a]From reference 7.
[b]Sheet failure in end bay without doubler plate.
[c]Ratios are based on values in columns indicated.

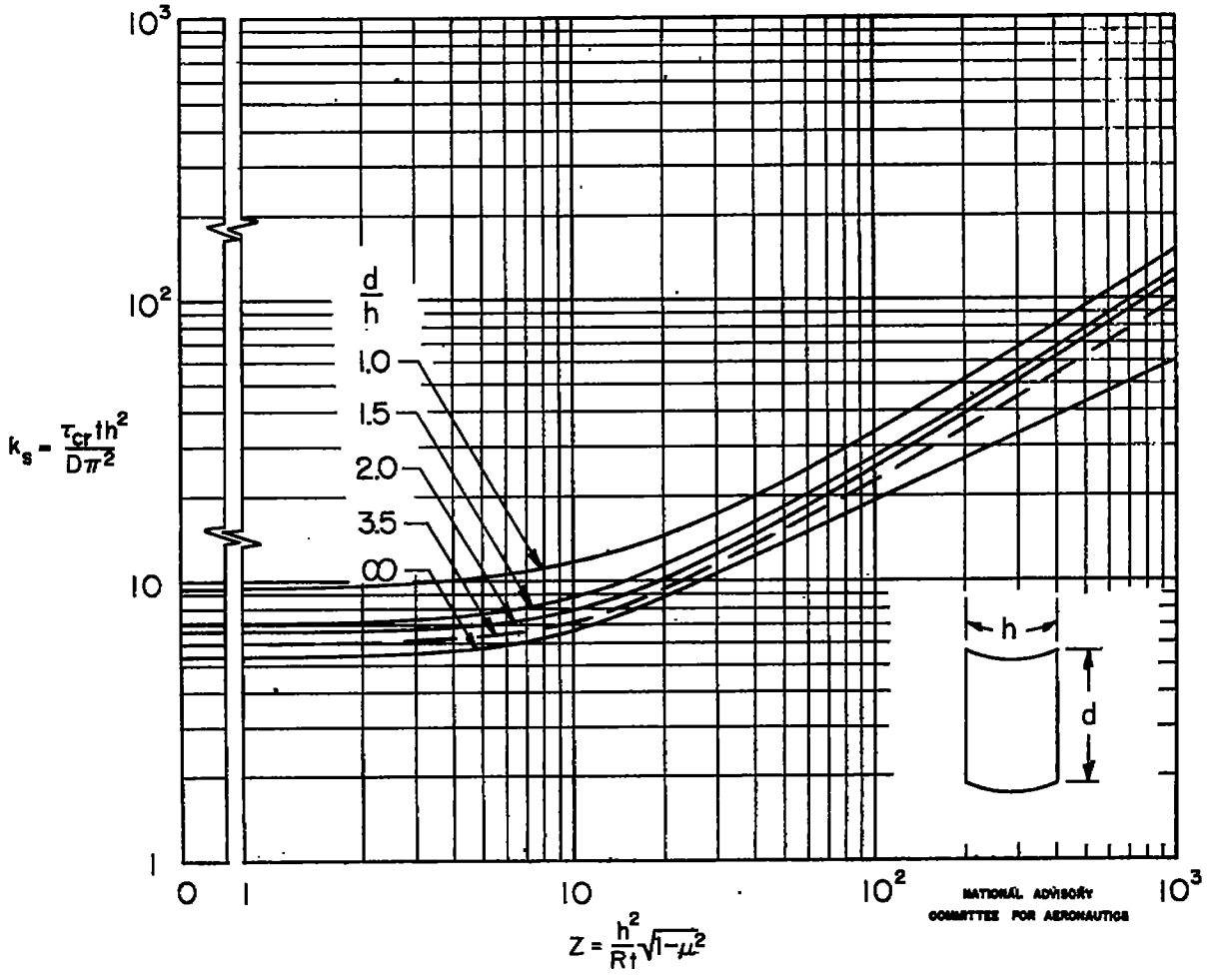

(a) $d \geq h$.

Figure 1.— Critical-shear-stress coefficients of simply supported curved panels.

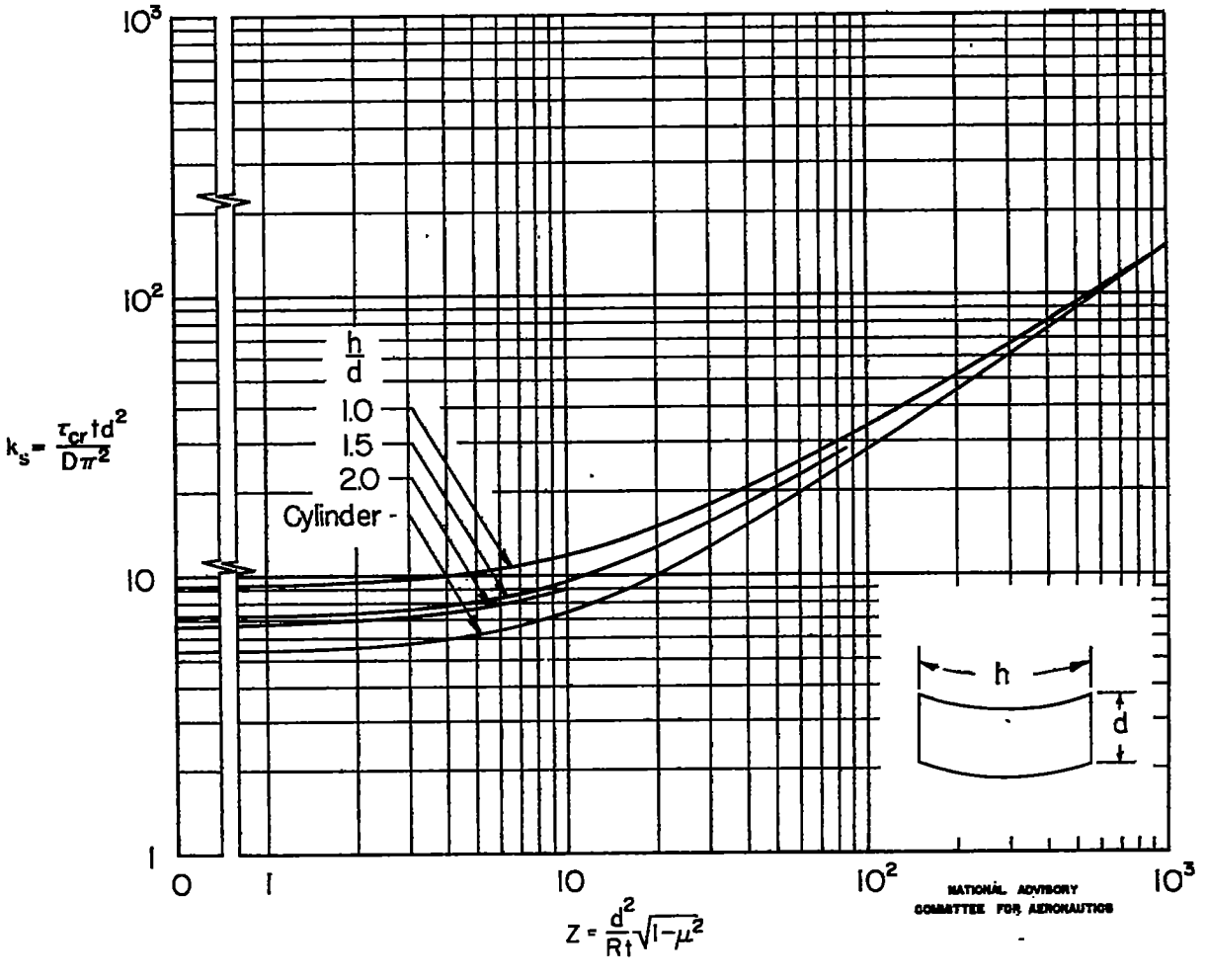

(b) $h \geq d$.

Figure 1.— Concluded.

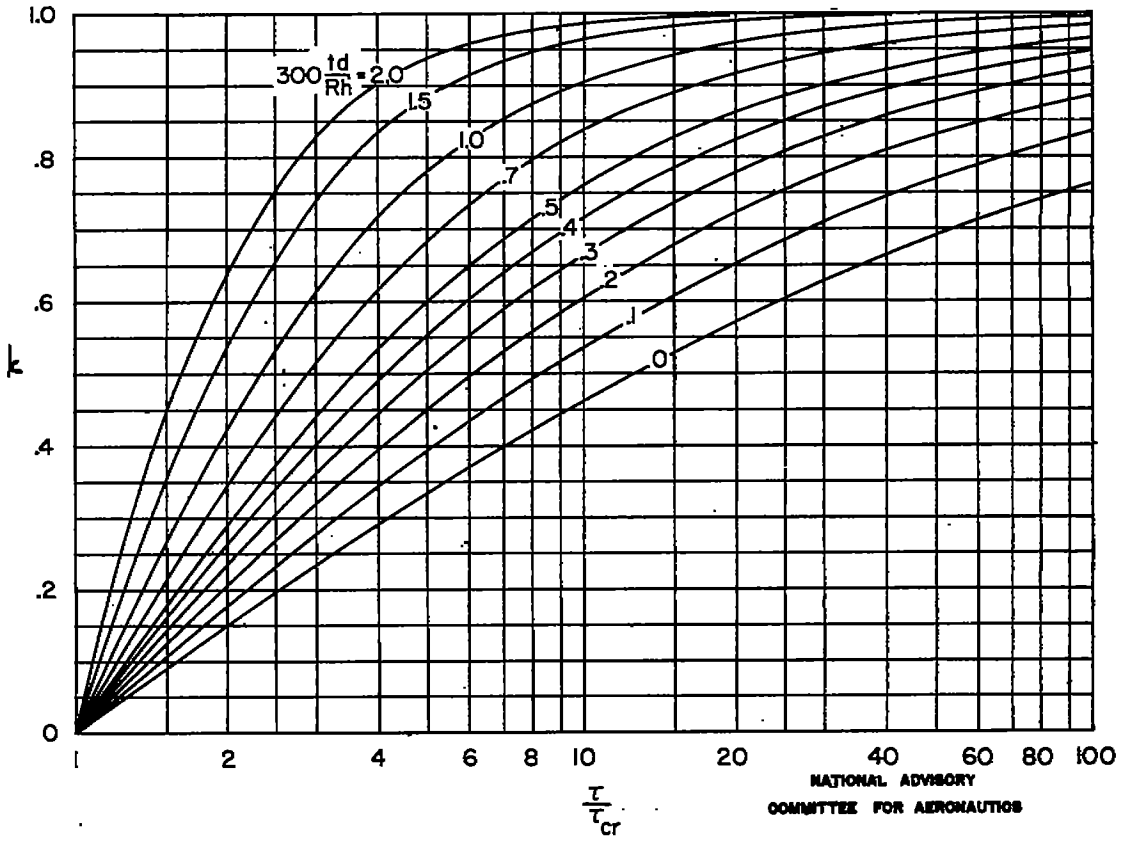

Figure 2.— Diagonal-tension factor k.

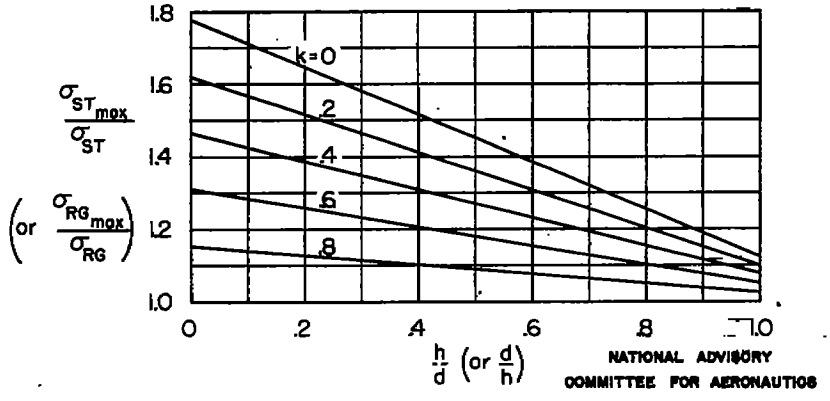

Figure 3.— Ratio of maximum stress to average stress in stiffeners.
(From reference 2.)

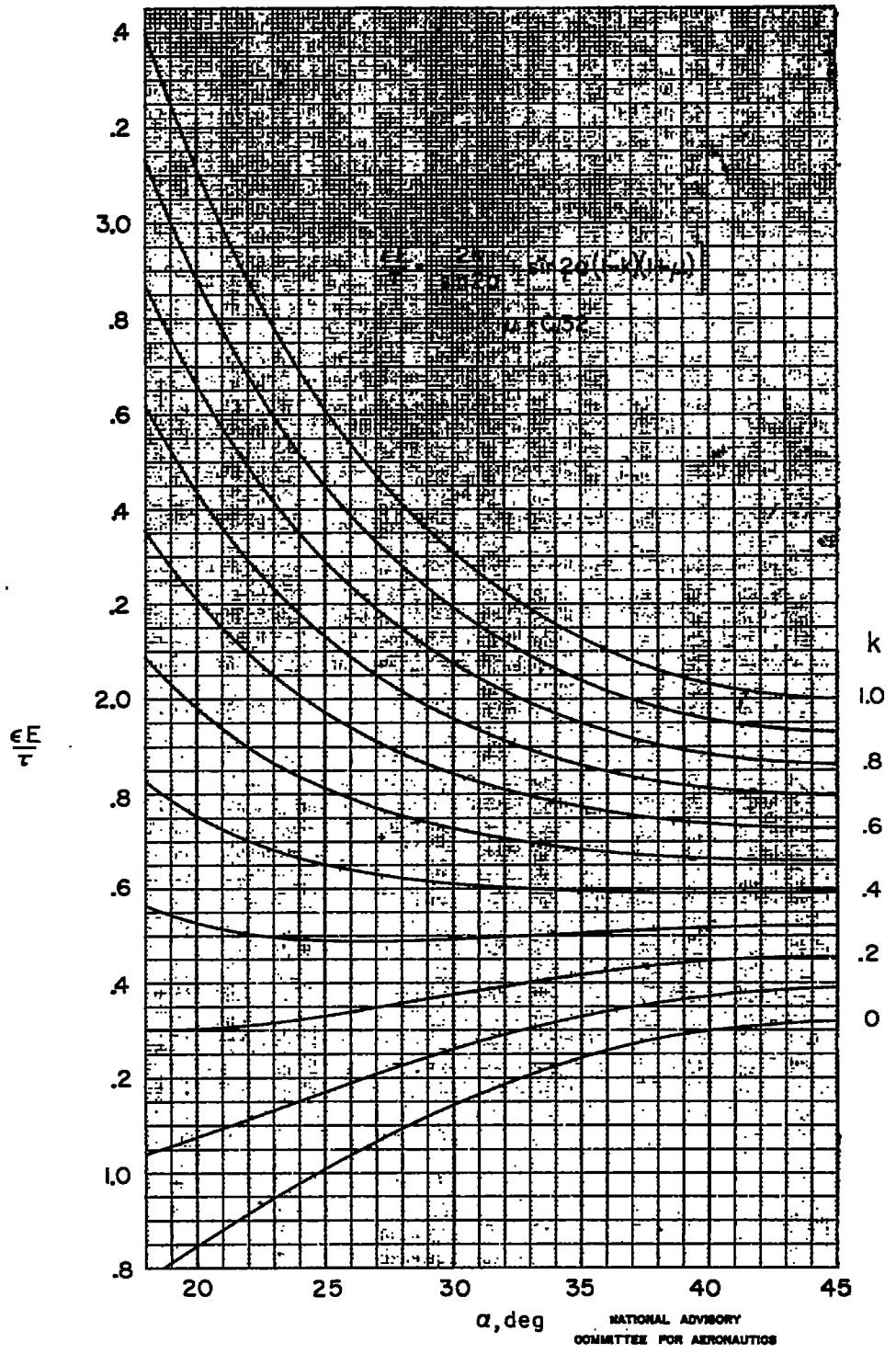

Figure 4.— Chart for obtaining ϵ.

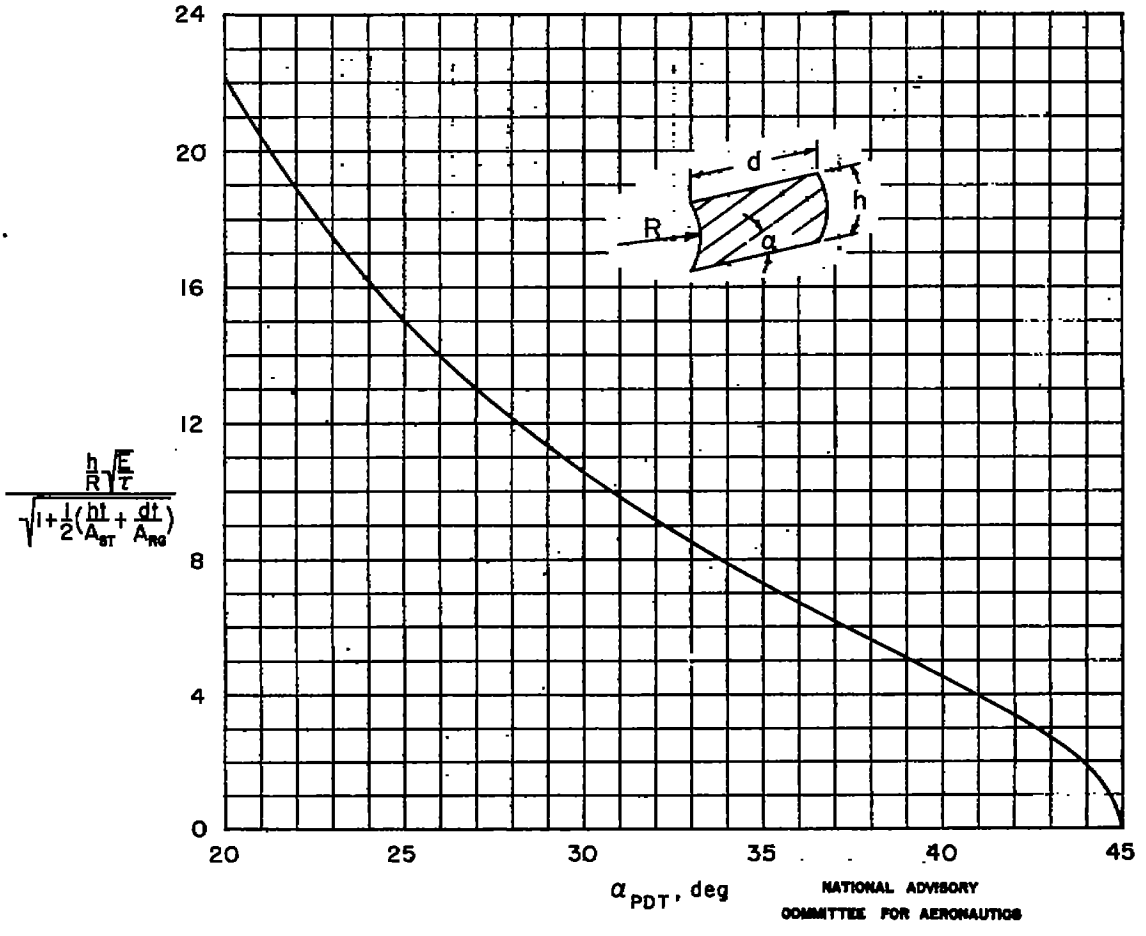

Figure 5.— First approximation of the angle of folds (based on pure diagonal tension). (Strictly valid only when $\frac{A_{ST}}{ht} = \frac{A_{RG}}{dt}$.)

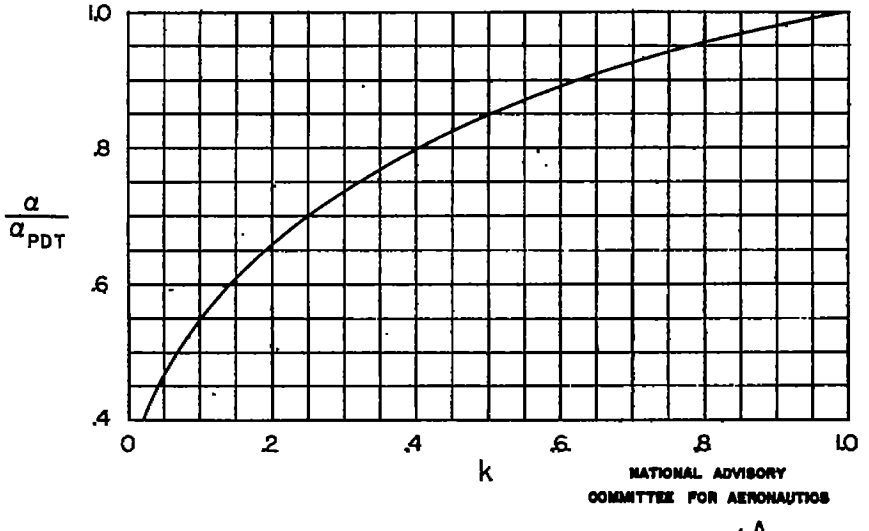

Figure 6.— Correction to first approximation of the angle of folds $\left(\frac{A_{ST}}{ht} = 1.00 = \frac{A_{RG}}{dt}\right)$.

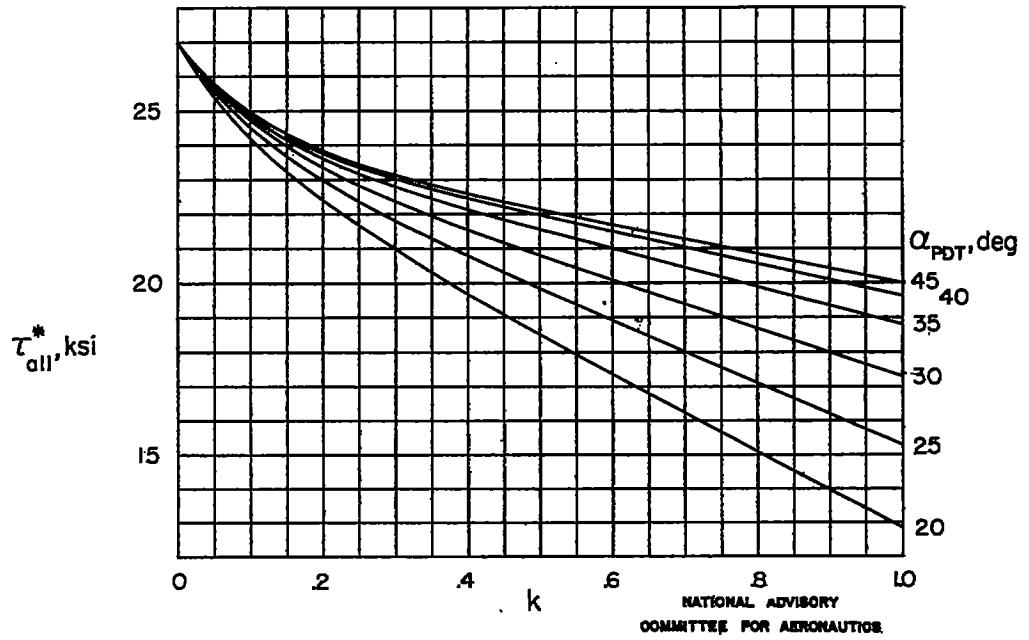

Figure 7.—Basic allowable shear stress τ^*_{all} for 24S-T aluminum alloy. σ_{ult} = 62 ksi.

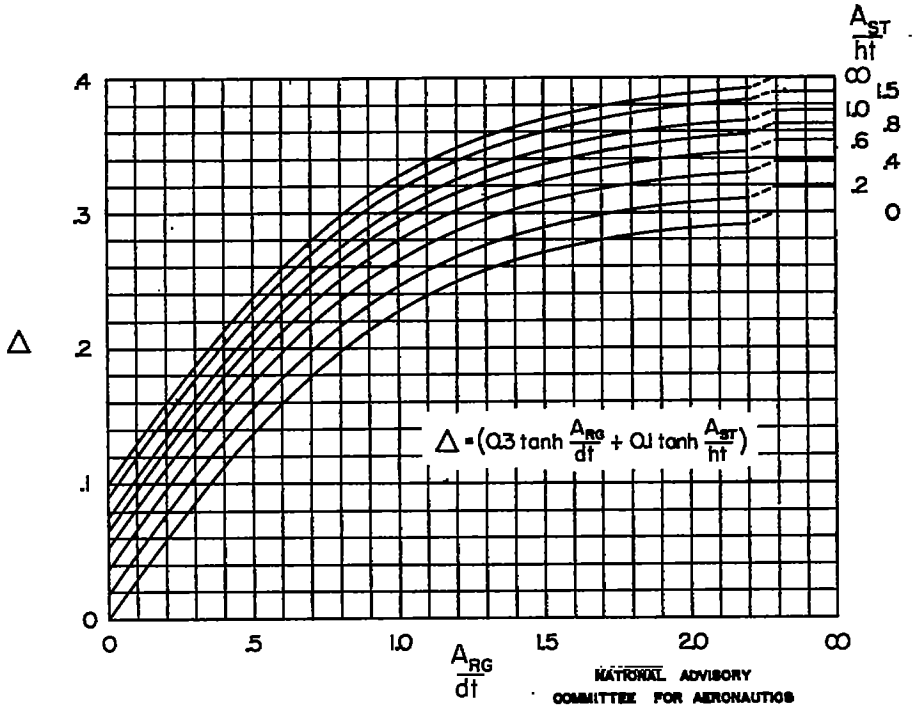

Figure 8.—Correction factor (due to effect of stiffeners) for allowable shear stress.

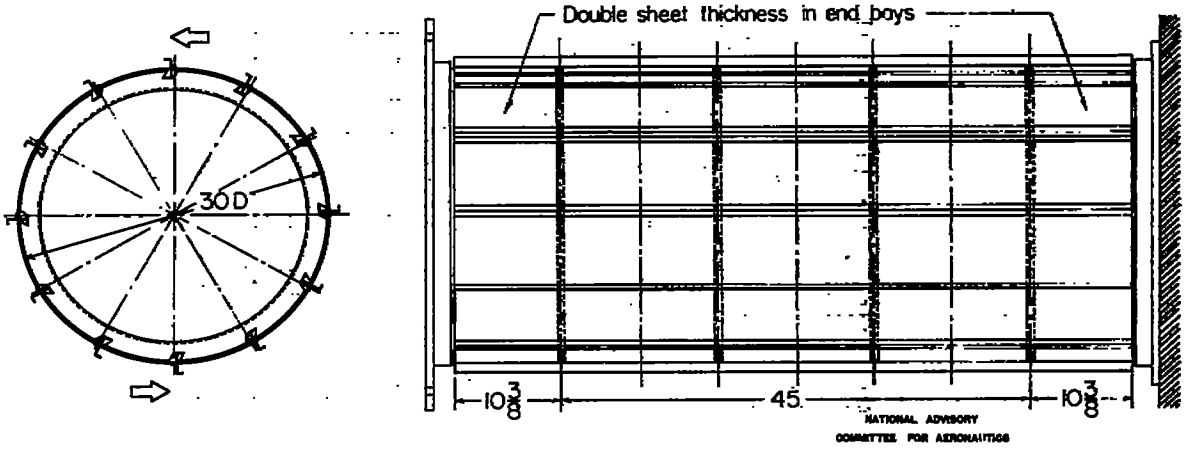

Figure 9.—Over-all dimensions of test cylinders.

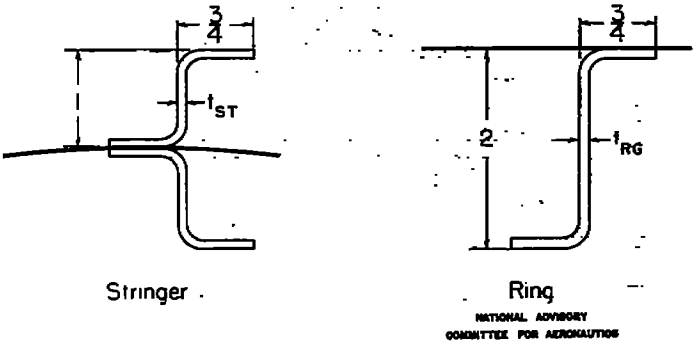

Figure 10.—Nominal dimensions of test-cylinder stiffeners.

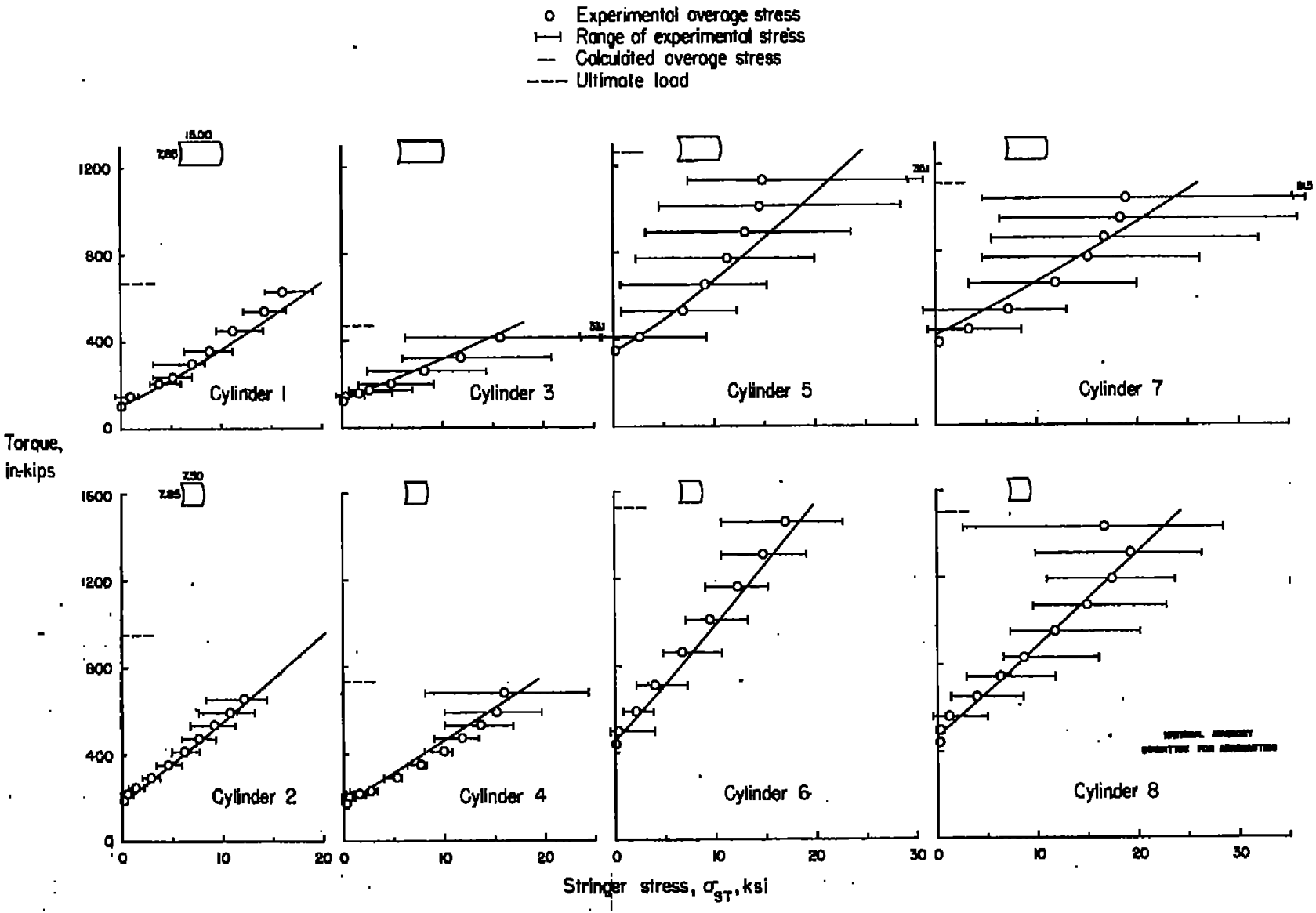

Figure 11.—Stringer stresses.

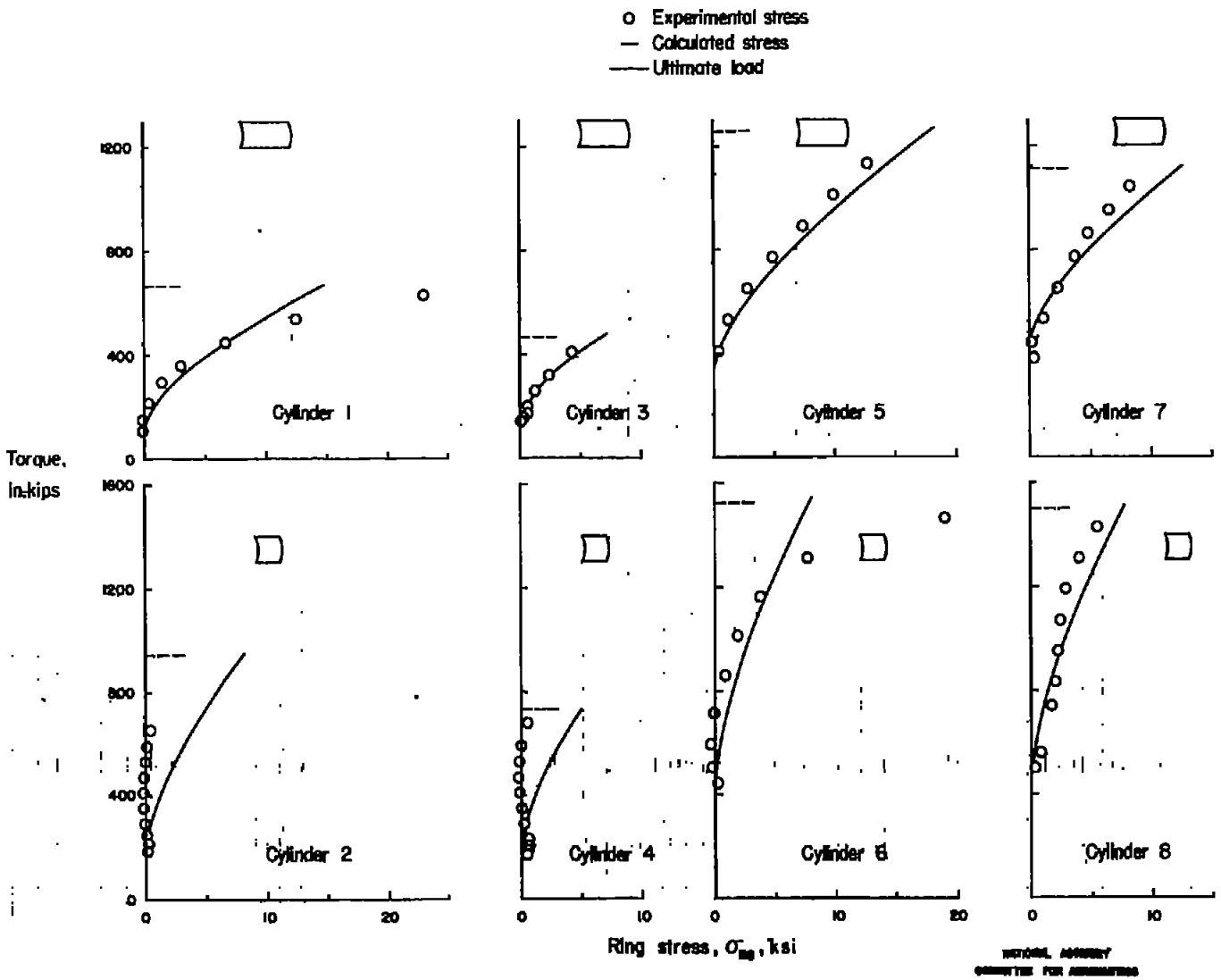

Figure 12.--Ring stresses.

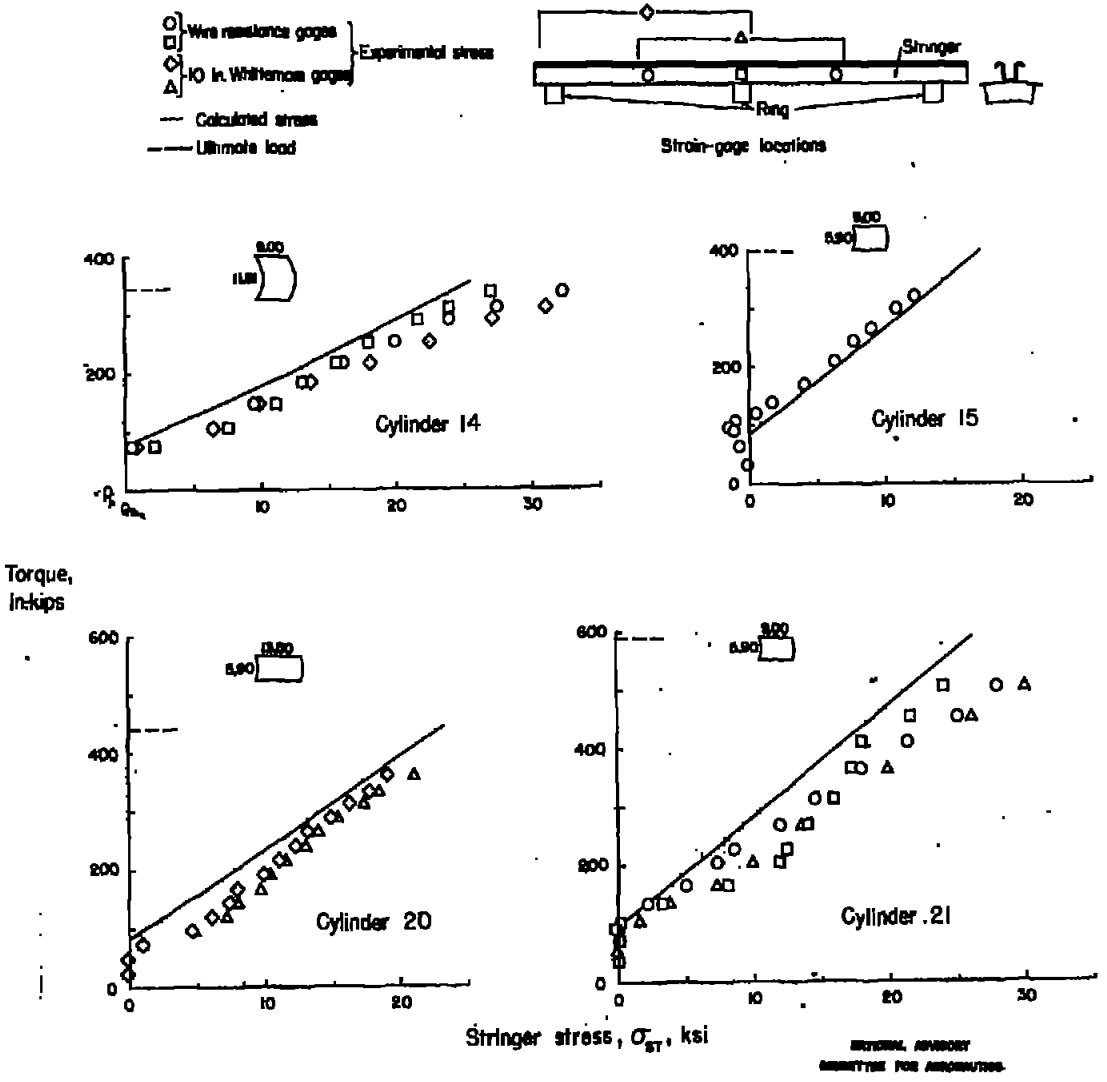

Figure 13.– Stringer stresses for test cylinders of reference 7.